Correlating Microgeometry to Slicing Mechanics (Continued)

A Major Qualifying Project Report

Submitted to the Faculty of
Worcester Polytechnic Institute

In partial fulfillment of the requirements for the
Degree of Bachelor of Science

By
Richard Kern
Dylan Flegel

Date:
April 27th, 2023

Report Submitted to:
Professor Christopher Brown
Worcester Polytechnic Institute

Abstract

The objective of this project was to investigate the relationship between ski sharpening method, ski edge geometry, and slicing depth. By investigating ski slicing, our research could provide insight into how different sharpening methods affect the severity of ski laceration injuries. These laceration injuries can be life-threatening. For our research, a ski was cut into segments that were each sharpened with a different method. The ski segments were then measured with a confocal microscope. To quantify the edge geometry for these measurements, both multiscale curvature analysis and power spectral density analysis were applied. To measure slicing performance, an apparatus was designed to slice a section of gelatin with each ski segment. The depth of each resulting slice was measured. The average slicing depth of each edge was then compared between sharpening methods. Additionally, slice depth was compared to the measured curvature across a range of curvature scales.

Foreword:

This is the second report of this MQP, with the previous report being titled "Correlating Microgeometry to Slicing Mechanics: Design of a Simulated Ski Laceration Machine". This was to allow one member, Dylan Flegel, to graduate in December of 2022. This involved detailing the design process of the machine used to test the slicing depth. Sections of writing from this previous report were reused for this final combined report.

Acknowledgments:

We would like to thank the WPI Surface Metrology Lab for providing the opportunity for this project and the WPI MQP Lab for providing access to 3D printers. We thank the WPI Ski Team for sharpening the ski edges. We also wish to thank Matt Gleason for providing Curfsoft, a software which will be used to analyze our ski edges during future work. We greatly appreciate the resources provided by Digital Surf, Sensofar, and Gel sight, which will also be used to measure and analyze our ski edges. Special thanks to Shu Guo for his continuous help with various aspects of this project. We would also like to thank the 9th International Conference on Science and Skiing for accepting our poster presentation of our research.

Table of Contents

List of Tables

List of Figures

1. Introduction

1.1. Objectives

This project attempts to investigate the relationships between ski sharpening method, ski edge geometry by multiscale curvature analysis, and slicing depth. This could provide insight into ski edge laceration injuries.

1.2. Rationale

Currently, there is little research investigating how the microgeometry of an edge relates to its slicing performance. By studying this relationship, insight into what microgeometries may be affecting the severity of laceration injuries could be provided. Additionally, the methods developed in this project could be used in future research to investigate the role of edge geometry in slicing mechanics.

It has been shown that lacerations caused by the edge of the ski can range between 5.6% to 33.6% of all skiing injuries, varying depending on the case study (Soares et al. 2022; Holden et al. 2022). The incidence of these injuries on a larger scale is still being studied. While these lacerations are uncommon, they can be life-threatening (Holden et al. 2022). Holden theorizes that the risk of ski laceration injuries could increase due to new mechanical sharpening methods. Such sharpening methods include the use of an EVO rotary mechanical sharpener (Figure 1). Part of this claim is that these sharpening techniques give "a serrated nature" to the edge, which "may generate burrs and unwanted ridges" (Holden et al. 2022). While this claim has not been proven, research has shown that blades with micro-serrations experience increased forces during slicing while also cutting deeper into soft material (Giovannini et al. 2016). Research into the microgeometry of ski edges may provide evidence of serrations caused by mechanical sharpening methods.

Figure 1: EVO rotary mechanical ski sharpener

1.3. State of the Art

A laceration is "a pattern of injury in which skin and underlying tissues are cut or torn" (Newman and Mahdy 2022), and can be caused by a wide variety of mechanisms. Ski lacerations, in this case, specifically refer to injuries caused by a ski edge cutting the skin and underlying tissue. Looking into the mechanics of cutting, Brown posits that there are three types of cutting: chopping, slicing, and scraping (Brown 2023). Like many real-world instances of cutting, ski lacerations can be a combination of all three cutting types. Predominantly, however, the mechanism of these lacerations can be described as slicing.

Slicing has been defined as a reduction in cutting force caused by motion parallel to the cutting edge. To explore the mechanics behind this reduction, Atkins defined the "slice-push ratio" (Atkins et al. 2004). This is the ratio between the velocity component parallel to the edge (slice), and the velocity component perpendicular to the edge (push). The slice-push ratio was compared to the parallel and perpendicular cutting forces, which were both normalized to the fracture toughness of the soft substrate.

With respect to the perpendicular cutting force, it was demonstrated that a linear increase in the slice-push ratio results in a non-linear reduction of the perpendicular cutting force. This decrease occurs as soon as horizontal movement is applied. With respect to the parallel force, it was found that applying movement parallel to the blade causes an increase in the parallel force until the slice-push ratio approaches one. After this peak, the parallel force slowly decreased as slice-push ratio was increased. Overall, this demonstrates that the slice-push ratio can describe how slicing reduces the forces required to cut a soft substrate.

Isolating the role of the slice-push ratio in the reduction in cutting forces has allowed further research into other factors that affect cutting forces. This included the examination of cutting angle. By comparing the expected reduction by the slice-push ratio to the measured reduction at various angles, it was found that the angle between an edge and its direction of motion can result in reduced cutting forces (Spagnoli et al. 2019).

1.1.1. Correlation of edge to performance

Microgeometry is a term specified by Denkena and Biermann to describe an edge. Specifically, microgeometry refers to all geometric detail that falls within the intersection between the two faces of an edge (Denkena and Biermann 2014). A visual representation of this definition is shown in Figure 2.

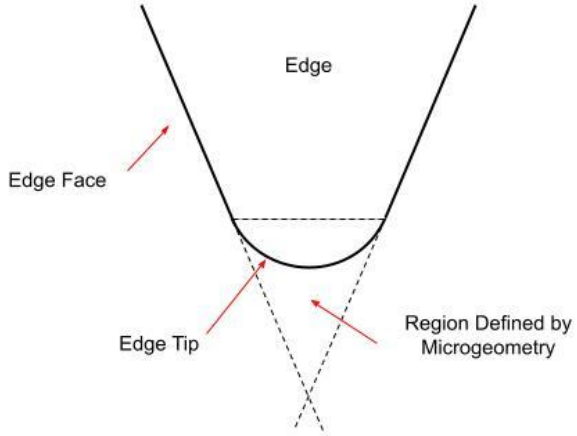

Figure 2: Microgeometry as Specified by Denkena and Biermann

Investigations correlating edge microgeometry to scraping performance have been well documented. For scraping, edge performance refers to the resulting chip formation. This research has shown that microgeometry determines all aspects of scraping mechanics, including cutting parameters, tool parameters, and scraping procedure (Denkena and Biermann 2014).

The correlation of edge microgeometry to chopping performance has been investigated. While a standardized definition of chopping performance has not been generally accepted, McCarthy proposed the use of a Blade Sharpness Index (BSI). This value is determined by measuring both edge displacement and cutting force required to initiate a cut into a soft substrate with known fracture toughness and thickness (McCarthy et al. 2007). Additionally, the cutting force can be written as a function of displacement once empirical constants are determined for a given material. The resulting measurement is independent of substrate properties, allowing further research to be done into what edge microgeometries affect BSI. Of the variables studied, it was found that the tip radius of an edge has the biggest impact on BSI. While the existence of a correlation was determined, further research is needed to correlate cutting performance to microgeometry accounting for measurement scale (McCarthy et al. 2010).

Correlations have been found relating microgeometry to both scraping and chopping performance. However, this is not the case for slicing. While research has been done into the mechanics of slicing, no correlation between edge microgeometry and slicing performance has been found (Deibel et al. 2013; Porazzo et al. 2017). Certain geometries have been shown to affect slicing performance, such as

a serrated scalpel studied by Giovannini. Despite this, there are a lack of generalized principles to predict slicing performance based on edge geometry. The fact that other mechanisms of cutting are directly affected by edge geometry suggests that such a correlation does exist.

1.1.2. Multiscale Analysis of Surface Topography

Surface topography is defined as the collection of locations of a surface (Brown et al. 2018). To characterize topography, a variety of methods have been developed. An important part of this characterization process involves "determining the scales of the different interactions" as "knowing the scales of interactions for topographically related phenomena is important" (Brown et al. 2018). In other words, surface topography can be characterized at a variety of different measurement scales. The scale where the surface topography interacts to cause the phenomena of interest is not always known beforehand. For example, the scales of measurement where the geometry of an edge may affect the slicing performance of that edge isn't known. A measurement scale that is too large could lose important details, while a measurement scale that is too small may measure variations too minor to impact slicing performance. Therefore, in order to determine how edge geometry affects slicing performance, multiple scales need to be analyzed. Despite the importance of considering the scale of measurement, many measurement parameters do not take scale into account. This has resulted in many "traditional parameters appear[ing] to lack systemization", making it "often unclear which parameters might be useful for a given situation" (Brown et al. 2018).

1.4. Approach

It is known that edge microgeometry directly influences the performance of other cutting mechanisms (McCarthy et al. 2010). Despite this, there is still a lack of general evidence correlating edge microgeometry to slicing performance. Accordingly, there is also a lack of evidence supporting the hypothesis that certain ski sharpening methods can increase the severity of laceration injuries.

To test different ski sharpening methods, a set of seven different ski segments was used. These segments were produced prior to this project at the WPI Surface Metrology Lab. Each segment was sharpened by hand with a file or using an Evo mechanical sharpener. The resulting topography of each ski edge segment was then measured with a Sensofar S Neox 3D optical profiler microscope. These ski segments were cut, sharpened, and measured prior to this project.

Multiscale analysis methods were used to measure the geometry of each ski edge. One analysis method selected to measure edge geometry multiscale curvature analysis (MCA). MCA involves the application of Heron's formula, which measures curvature based on the inverse radius of three points on a cross-section, with the scale of the measurement being "determined by the horizontal distance between the two corner points" (Figure 3) (Stemp et al. 2019). When the top-most angle of measurement between the three points is less than 90°, calculations are instead completed using a separate calculus derivative method (Stemp et al. 2019). Curvature was measured across a variety of different scales because the measured curvature of a surface varies as the scale of measurement changes (Brown et al. 2018). Additionally, the scale of interaction between edge geometry and slicing performance was not known prior to this research.

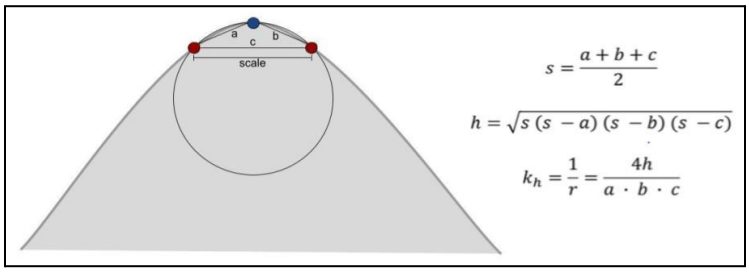

Figure 3: MCA Illustration with Equations (Stemp et al. 2019)

Another analysis method that was selected to measure geometry was power spectral density (PSD). This has been previously used as a measure of surface roughness and spatial frequency (Jacobs et al. 2017, Brown et al. 2018). This method was selected to measure spatial frequencies along the ski edge. The resulting measurement consists of the amplitude of each frequency contributing to the measured geometry. Comparisons could then determine whether certain sharpening methods caused repeated serrations along the edge. While not traditionally considered a multiscale analysis method, PSD "provides an evaluation of the magnitude of each scale" of frequency measurement (Brown et al. 2018). This measurement of multiple frequencies indicates that this analysis method is multiscale.

In order to measure slicing performance, our team designed and constructed an apparatus to slice a gel substrate with each ski edge segment (Flegel and Kern 2022). To design this apparatus, we applied axiomatic design principles. The first axiom is maintaining independence. By establishing design requirements and solutions that are each independent from one another, elements of the resulting design can be easily adjusted. This is because adjusting one element will not infringe on separate elements of the design. Suh's second axiom is minimizing information. This helps ensure simplicity in the final design, maximizing its probability of success. Throughout the axiomatic design process, multiple design parameters are devised for each identified functional requirement. The most viable design parameter is then selected.

2. Methods

2.1. Measuring Slicing Performance

Our team built an apparatus that can slice a piece of gelatin using ski segments (Fig. 4) (Flegel and Kern 2022). The machine operates by sliding a piece of gel over a ski edge. A weight is placed above the gel, pushing the gel into the edge. The apparatus allowed the team to slice gel with a reproducible speed and force.

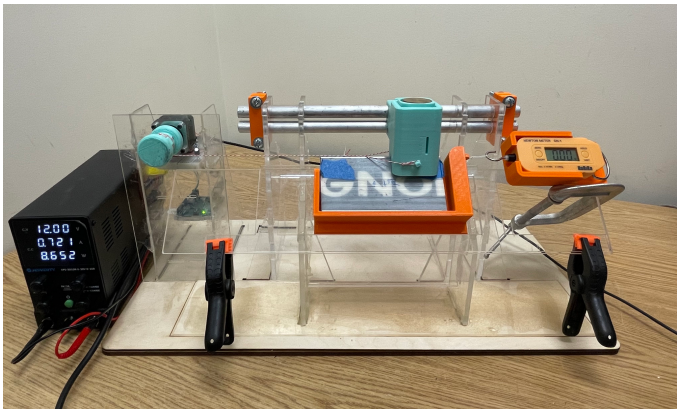

Figure 4: Slicing Apparatus

The code was calibrated to satisfy the parameters of the trials. The length of the ski segments would vary in length by about 1". The machine was programmed to move the gel the length of the smallest ski, which was 4". The speed of the motor is inversely proportional to the torque, so the motor was set to the fastest speed that could maintain sufficient torque to move the gel housing across the ski. The code is shown in Appendix A.

The gel used to represent skin was 33% gelatin and 67% water (Moronkeji, 2017). A variety of ratios were tested. Too little gelatin resulted in the gel crumbling under the weights, while too much gelatin would result in a gel too stiff to be sliced. When creating the gelatin, it was important the gelatin powder was fully dissolved into the water. To ensure the gelatin was evenly mixed, the gelatin was mixed in a double boiler system so it would be continuously heated. Once the gelatin was dissolved the system was weighed to determine how much water had evaporated during the process, this water was added back

in to ensure the ratio between gelatin and water was consistent. The gel was then poured into a baking sheet. The baking sheet and gel were covered and placed in a container with a small amount of water at the bottom. This was done to regulate the humidity of the container and mitigate the amount of water that evaporated from the gel. The container was then placed in a refrigerator to prevent mold. Three baking sheets of gel were made.

When it was time to conduct trials, the gel was taken out of the refrigerator approximately an hour and a half before testing. The gel becomes more rigid when cold, so it was important the gel was at room temperature when the trials were conducted. This ensures the material properties of the gel are consistent when sliced. Once the gel had reached room temperature, they were cut out of the baking sheets into 1" x 1.5" sections. A corner of the gel was then dyed to identify which direction the gel was being sliced.

Seven ski segments were tested. Three were sharpened with a file by hand, and four were sharpened with the EVO sharpener. Finishing stones were also applied to each edge, except for edges F and G. Edge G was only sharpened with an EVO sharpener and edge F was only sharpened with a file. Six pieces of gel were sliced with each edge using the slicing apparatus. There were three containers of gel from the same mixture. Six trials were conducted for every edge. This involved slicing two gels from each container. This was done to ensure any slight inconsistencies in gelatin concentration between containers did not skew the data. Glycerin was used as lubricant and was applied to the edge before each trial. The guide rails on the apparatus were also lubricated.

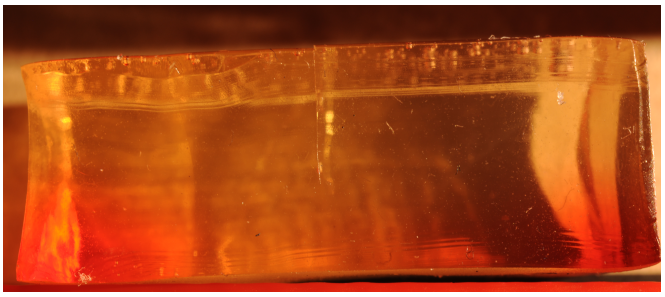

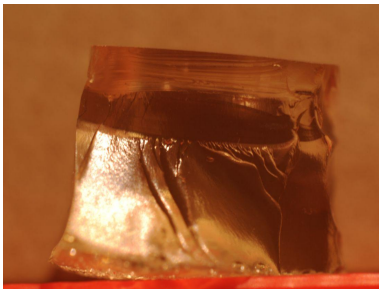

Figure 5 (left): Side view of gel slice
Figure 6 (right): Fractured view of gel slice

Each gel was photographed with a macroscopic lens. The resolution of these photos were 4288px X 2848 px. One pixel was about 7µm. One picture was taken for each side, resulting in two photographs for every trial. A photograph of the slice is shown in Figure 5. The slice in each photograph was analyzed to determine the slice depth. The vertical distance was measured from the gel surface to the bottom of the slice. When the gel surface was uneven, two measurements were taken on a single side and averaged together. An illustration of this with an exaggerated difference in depths is shown in Figure 7. The depth measurements for each side were then averaged together to calculate the depth cut per trial. This slicing depth was recorded to a precision of 0.1 mm. Some gels were fully separated in half after the trail to examine the inside surface of the cut produced by the slice. The gel was fractured so it was clear which region was sliced by the edge. This is shown above in Figure 6. The top region was sliced by the ski, and the bottom region was fractured after the trial.

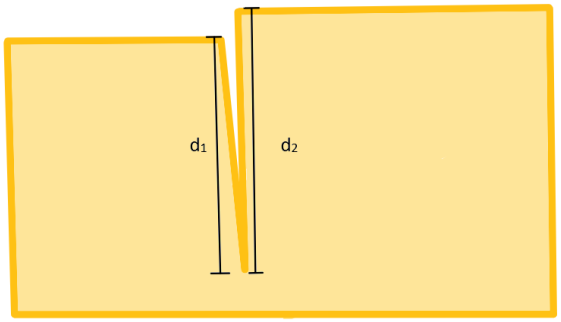

Figure 7: Illustration of Slice Depth Analysis

2.2. Analyzing Edge Topography

Each ski edge segment was measured at x5 magnification with a Sensofar S Neox 3D optical profiler microscope at a sampling interval of 2.76µm. The measurements were taken before the slicing trials. The data was analyzed in MountainsMap. Non-measured points were filled. An example measurement is shown in Figure 8. An algorithm was made to define where the edge was located on the edge measurement. It worked by finding the highest point for each y-coordinate. A line of best fit was created using the highest point from each row. This line was the profile used to define the edge. A figure showing the highest points and the line of best fit is shown in Figure 9. After the profiles were defined, they were all leveled. The code used for the process is shown in Appendix B.

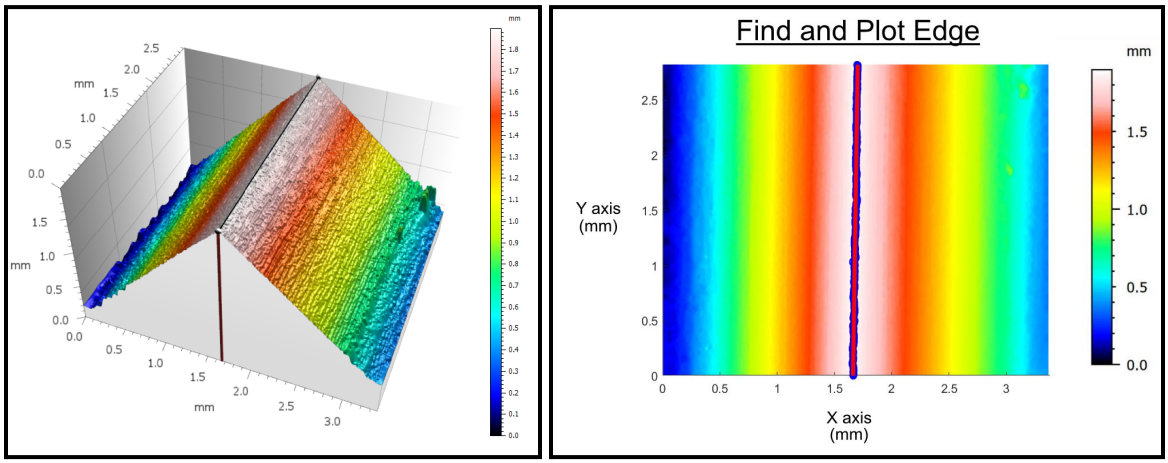

Figure 8: Filled Non-Measured Points in MountainsMap
Figure 9: Highest Points and Best Fit Line on Edge

The measurements were rotated such that the line of best fit was vertical. For each measurement, three cross sections were then defined as horizontal profiles perpendicular to the edge (Fig 11). An example cross section profile is shown in Figure 11.

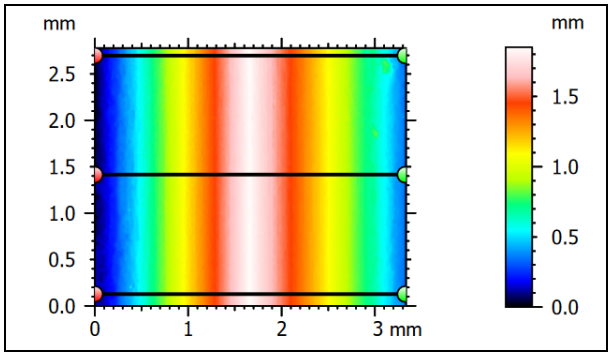

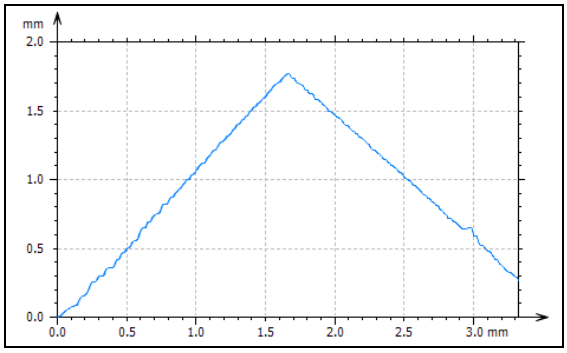

Figure 10: Three Cross Sections Perpendicular to Edge
Figure 11: Cross Section Profile Example

Multiscale curvature analysis (MCA) was applied to each cross section. This was done using Curvsoft, a software developed at the WPI Surface Metrology Lab by Matt Gleason (Stemp et al. 2019). The curvature at the highest point of each edge cross section was used for the analysis. This was recorded for every scale. These values are compared to the slicing performance of the edge.

The curvature could not be calculated at the highest point of the edge cross section. This is because at the highest scales, only the points directly in the center could be calculated. The center did not always line up with the highest point of the edge. Trimming the data to center the highest point would reduce the amount of scales able to be calculated. Therefore, the highest scales between 3124.32 µm and 3375.48 µm were not used for the comparison between curvature and slicing performance. Excluding the largest scales would not significantly impact the results as these scales are likely too large to describe how the geometry will affect the performance.

Power spectral density analysis (PSD) was applied to the edge profiles using MountainsMap. PSD is able to characterize the frequencies of the surface geometry. Observing the strength of these frequencies could indicate if there were more microserrations on edges sharpened with an EVO mechanical sharpener.

3. Results

The slicing depths for the 6 trials were averaged together to calculate the average slicing depth produced by each edge. The results are shown in Table 1. The difference between the average depth sliced by an edge sharpened by hand and the average depth sliced by an edge sharpened with an EVO sharpener was 0.2mm. The standard deviation for the trials conducted with edges sharpened with an EVO was 1.4. The standard deviation for the trials conducted with edges sharpened by hand was 1.7. The data is also shown as a bar graph in Figure 12. The error bars represent one standard deviation for each edge.

Evo Sharpened	**Depth (mm)**	**Hand Sharpened**	**Depth (mm)**
Edge A	5.2	Edge D	4.5
Edge B	5.6	Edge E	6.2
Edge C	4.8	Edge F	5.4
Edge G	5.1		
Mean	5.2		5.4
Standard Deviation	1.4		1.7

Table 1: Slicing Depth of Edges

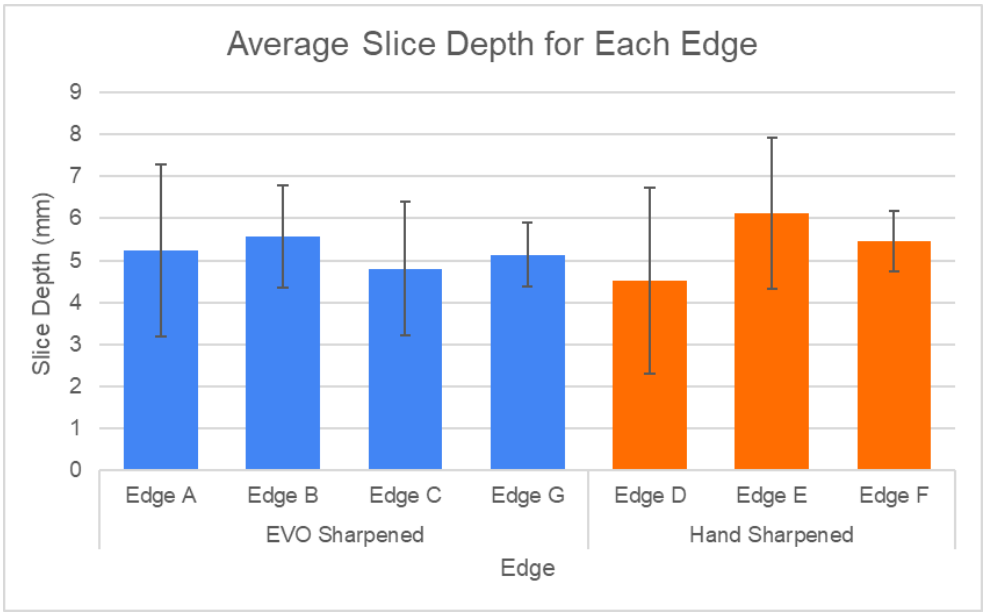

Figure 12: Slicing Depth for Edges with 1 Standard Deviation

For every edge, 6 PSD graphs were generated. Example PSD graphs are shown below in Figure 13. All 45 PSD graphs are shown in Appendix C. The arrow points to the peak amplitude. This indicates the strongest frequency present in the edge profile.

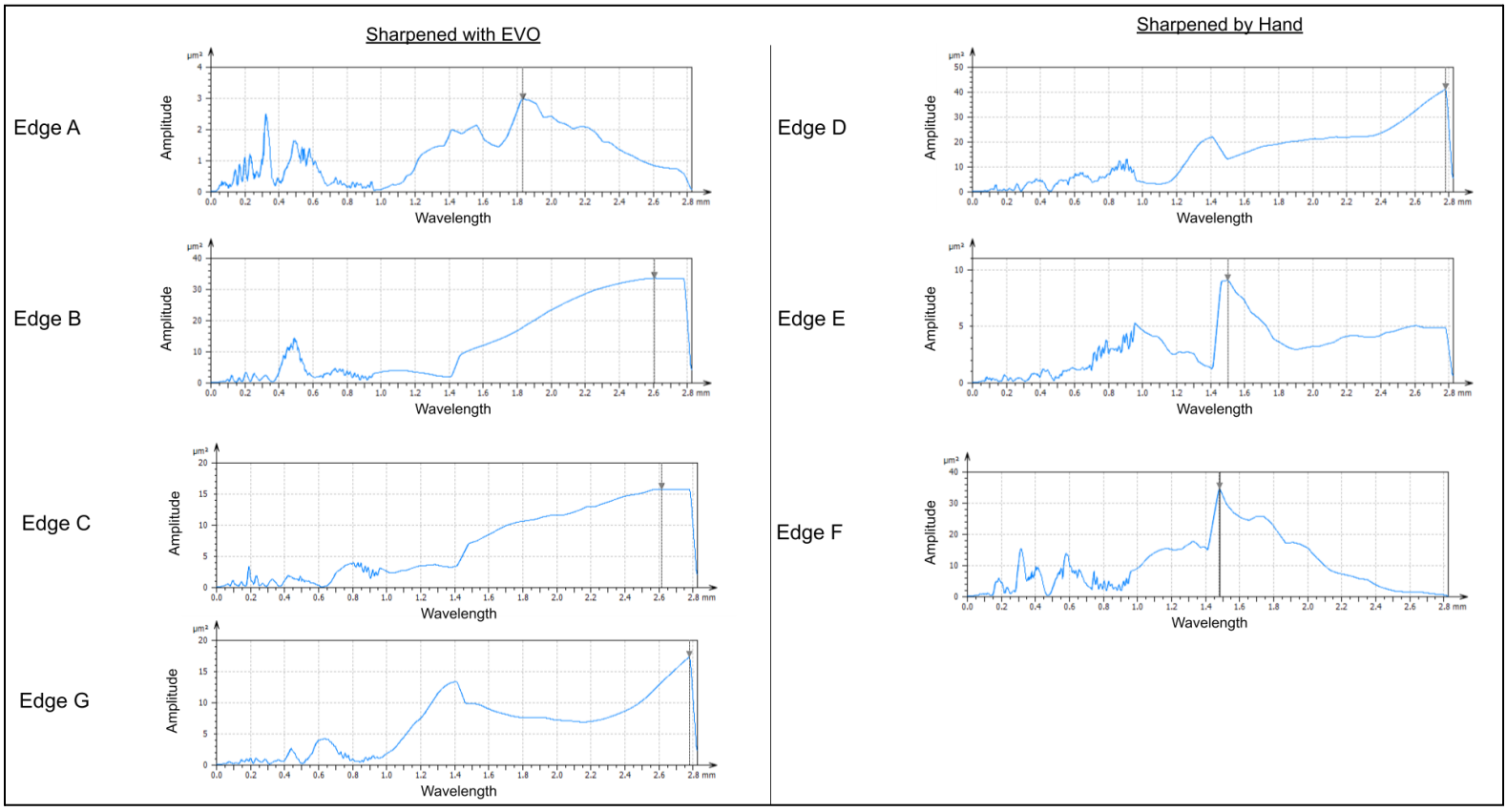

Figure 13: Example PSD graphs

A graph showing the curvature values at each scale is shown in Figure 14. This was completed by analyzing a single edge cross-section with CurvSoft and exporting the resulting curvatures to MountainsMap. Scale increases from left to right, with each row representing the curvature at one scale. The height of each point is the curvature value. The larger the scale of measurement, the fewer number of measurements could be taken.

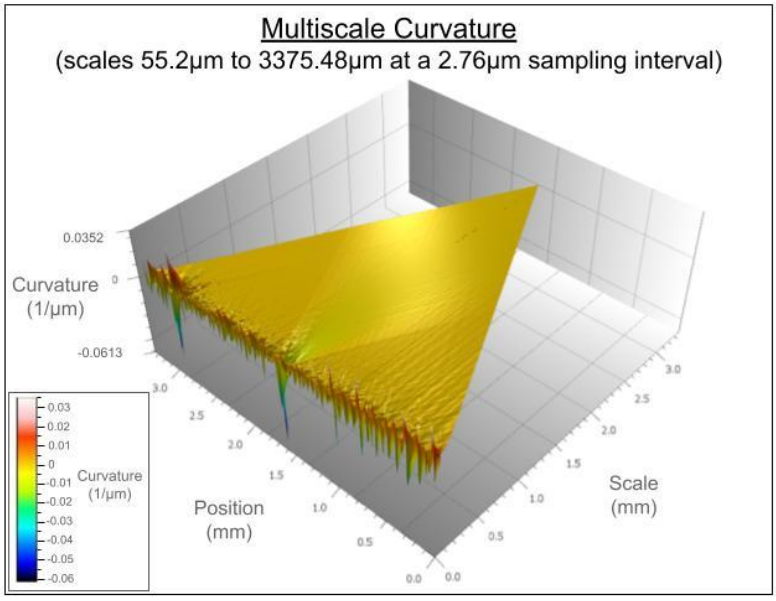

Figure 14: Multiscale Curvature Plot of Edge: All Scales

For every scale, the curvature at the highest point of each edge cross section was recorded. These curvatures were then compared to the depth produced by the edge. An example graph for a curvature scale of 237.36µm is shown below in Figure 15; each point represents one edge. The line of best fit was generated and the correlation coefficient was calculated. A correlation coefficient (R) was found for all 564 scales ranging from 5.52µm to 3118.8µm. The R value for every scale was plotted in the scatterplot below in Figure 16.

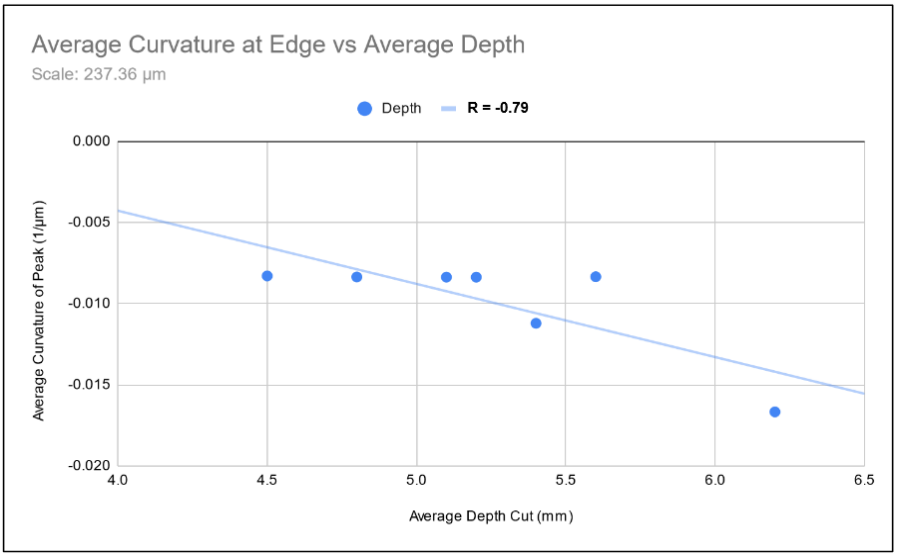

Figure 15: Example Curvature at Edge vs Average Depth

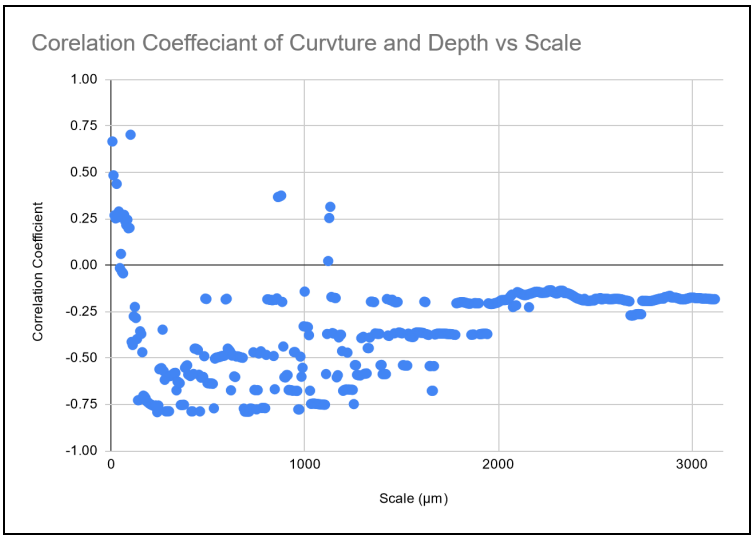

Figure 16: Correlation Coefficient of Curvature and Depth vs Scale

4. Discussion and Conclusions

Overall, our team was unable to discriminate sharpening method based on slicing depth. Comparing the slicing depths of edges sharpened with an EVO sharpener to edges sharpened by hand showed no significant difference between sharpening method. We were also unable to discriminate sharpening methods based on PSD. It remains inconclusive whether EVO sharpening increases microserrations. Despite this, significant correlations between edge curvature and slicing depth were found at certain curvature measurement scales.

4.1. Sharpening Method and Slicing performance

Our team was successfully able to measure the slicing performance of ski edges sharpened with different methods. The difference in average slicing depth between skis sharpened by hand and skis sharpened with an EVO mechanical sharpener was 0.2 mm (Table 1). The standard deviation of each method was 1.7 mm for skis sharpened by hand and 1.4 mm for skis sharpened with an EVO sharpener. Based on these slicing depth measurements, no significant difference between sharpening method could be found. This means that our trials were inconclusive in determining whether either sharpening method results in a ski edge that slices deeper into a soft substrate.

4.2. Sharpening Method and Power Spectral Density (PSD)

The power spectral density (PSD) of edges sharpened with an EVO mechanical sharpener to edges sharpened by hand were compared. Based on 45 PSD graphs (Figure 14 and Appendix C), no relationship between sharpening method and the resulting PSD analysis could be found. Consequently, this comparison was inconclusive in determining whether EVO mechanical sharpening methods cause an increase in microserrations. This conclusion was largely based on the fact that no consistent relationship between sharpening method and the resulting PSD graph could be found. The comparison was also inconclusive about whether the PSD graphs provided any evidence of microserrations along each edge.

4.3. Multiscale Curvature Analysis (MCA) and Slicing Depth

The correlation between slicing performance and the curvature of the edge was determined for curvature measurement scales between 5.52µm and 3118.8µm. The resulting graph between curvature scale and the associated correlation showed distinguishable regions of correlation based on scale (Figure 17). This supports existing literature by demonstrating that curvature is a scale-sensitive analysis

parameter (Stemp et al. 2019; Brown et al. 2018). In other words, curvature is only related to slicing depth at certain scales of interaction.

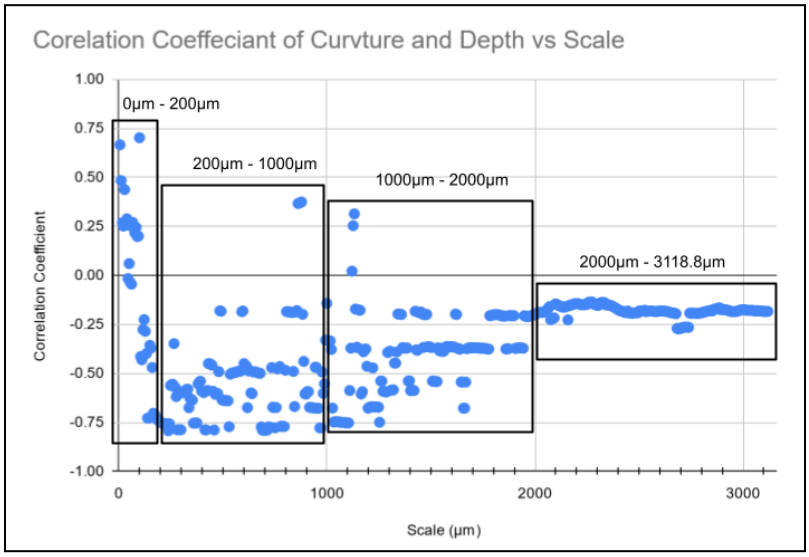

Figure 17: Correlation Coefficient of Curvature and Depth vs Scale with Regions

The strongest correlations were found between scales 200µm-1000µm. This included the strongest correlation between curvature and slicing depth. This correlation was -0.79, which resulted from a curvature measurement scale of 237.36µm. Based on these correlations, we can conclude that measurements at these scales best describe how the curvature of an edge relates to slicing depth. Possible reasoning as to why this is the case can be seen in an example of curvature measurements from this region (Figure 18). In the figure below, the largest magnitude curvatures prominently display the position of the edge tip. The fact that the curvature at the edge peak is most prominent in these scales supports the finding that these scales best describe the relationship between edge curvature and slicing depth.

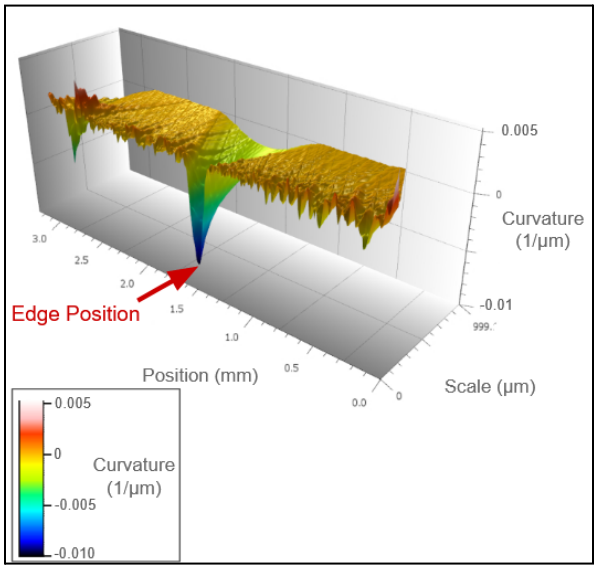

Figure 18: Multiscale Curvature Plot of Edge: Scales 200µm- 1000µm

At scales between 5.52µm-200µm, we found no strong correlation between curvature and slicing depth. An example displaying curvature measurements from this region shows significant noise at these smaller scales (Figure 19). At this scale, there is no noticeable trend in the data that could be correlated to slicing depth (Figure 17). This is likely what causes the correlation between slicing depth and curvature measured at this scale to vary wildly. This figure also illustrates why the edge geometry at this scale is likely too small to affect the depth of the slice.

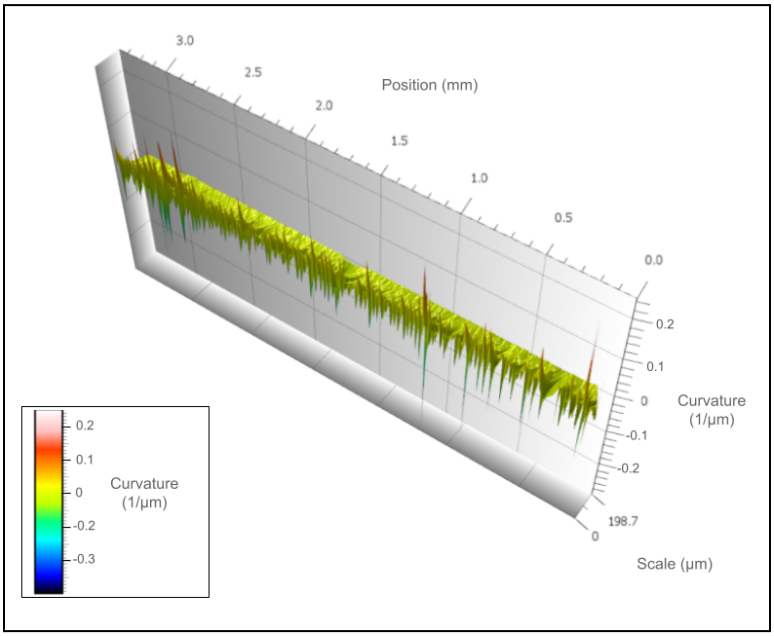

Figure 19: Multiscale Curvature Plot of Edge: Scales 5.52 µm - 200 µm

At scales between 1000µm-2000µm, the correlation between curvature and slicing depth began to decrease. An example displaying curvature measurements from this region shows the largest magnitude curvatures at the edge position (Figure 20). Despite this, the magnitude of these curvature measurements are significantly reduced. This reduction in magnitude may indicate why there is a reduced correlation between curvature and slicing depth.

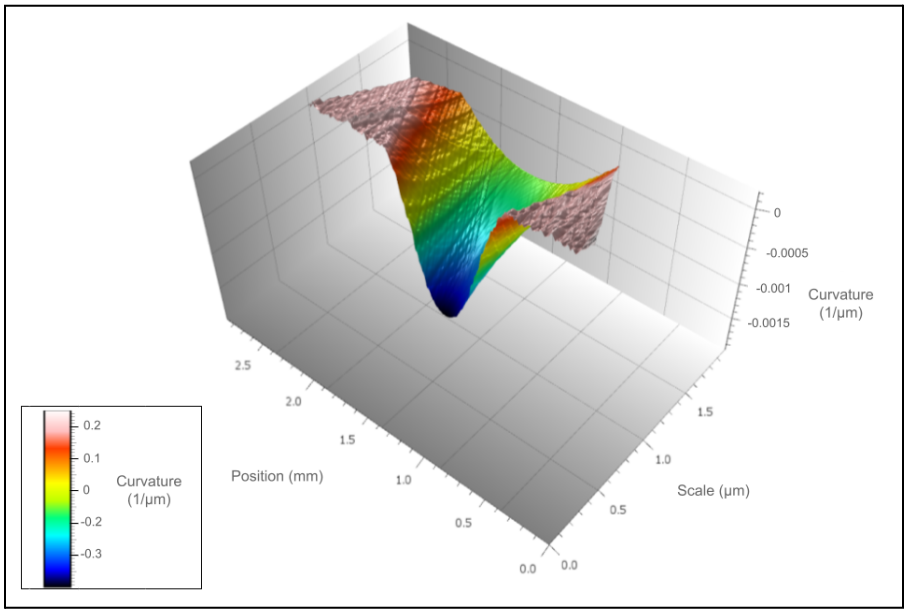

Figure 20: Multiscale Curvature Plot of Edge: Scales 1000- 2000µm

Between scales 2000µm - 3118.8µm, the correlation between curvature and slicing depth was consistently low. At these large scales, the correlation stayed consistently around -0.18 (Figure 17). This is likely because the relevant details of the edge are lost at these scales. As seen in the example curvature graph in Figure 21, most variation in curvature at this scale is less than a factor of 0.001µm.

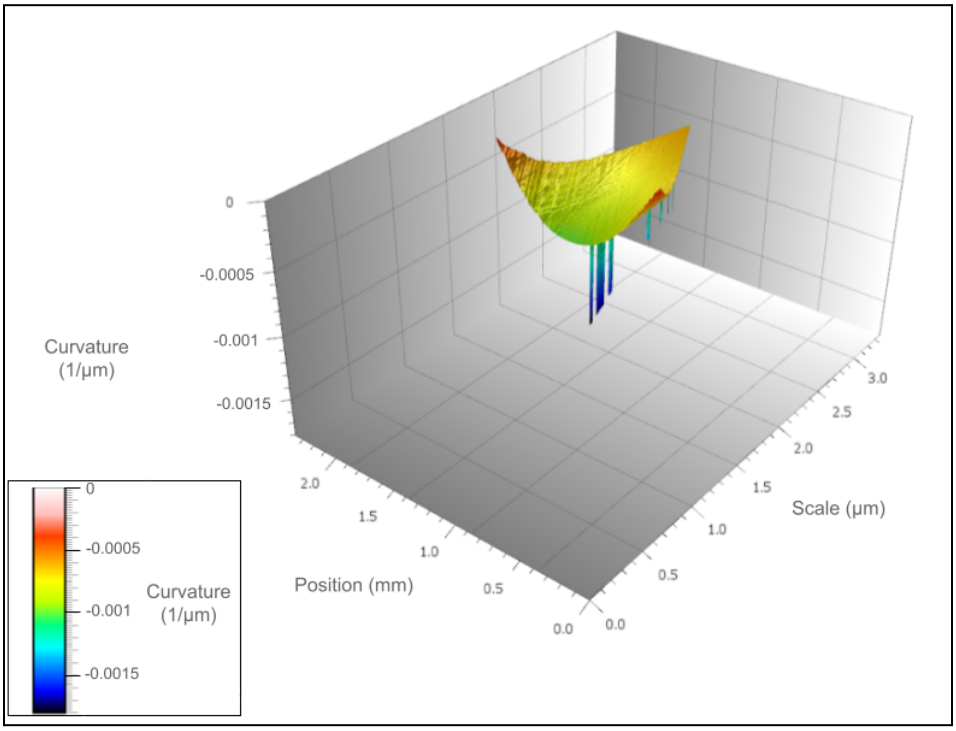

Figure 21: Multiscale Curvature Plot of Edge: Scales 2000µm - 3118.8µm

Ethics statement

First Canon of Engineering Ethics: *Hold paramount the safety, health and welfare of the public.*

Environmental:

Our project involved the design and fabrication of an apparatus that could test the slicing performance of ski edge segments. Throughout this process, it was beneficial to fabricate parts of the structure out of plastics. This included 3D printing parts to house a gel. This would be moved across the ski edge to produce a slice in the material. Using 3D printed PLA allowed this part to be lightweight, reducing the torque on our motor. This allowed for an increase in speed that was necessary to produce the required slice. Additionally, using 3D printed PLA gave us the ability to test different design prototypes in a limited amount of time. While using 3D printed PLA gave many advantages in our use case, our rapid prototyping produced plastic waste. Our apparatus also used a base fabricated out of laser-cut acrylic. This gave us a sturdy structure to hold the ski segment, while also reducing friction between the base and the ski. This allowed us to measure the friction forces acting on the ski. The laser cutting process, however, produced plastic waste. Future versions of the apparatus could replace the plastic parts with a more sustainable material. This could include fabricating parts out of aluminum through the use of a CNC machine. While the plastic waste generated during this project was relatively negligible, mass production of our apparatus should reduce the amount of plastic used. This would aim to reduce plastic pollution that disproportionately affects the health of marginalized communities.

Social:

The goal of this project was to investigate the relationship between ski edge geometry, sharpening method, and slicing performance. This may provide insight into how sharpening method affects the severity of laceration injuries caused by ski edges. As these laceration injuries can be life-threatening (Holden et al. 2022), research into the mechanics behind these injuries may lead to safer ski sharpening methods. While our research was not able to discern the sharpening method based on slicing performance, we only recorded slicing depth into a single type of soft gelatin substrate. Our current research could contribute to a general understanding of slicing mechanics. This could have multiple applications outside of skiing, including healthcare. Research into how sharpening methods affect an edges slicing performance could improve the effectiveness of surgical tools. Along with this research into surgical tools, measures should be taken into making effective sharpening methods affordable to avoid increasing healthcare disparities.

Global:

Studying how ski edge sharpening relates to a risk of laceration injury could increase the safety of the sport around the world. Such research would allow countries to increase the safety of their ski areas by enforcing the use of safer skis. While this benefits a limited number of countries, research into how edge sharpening affects slicing performance has applications in multiple industries. As mentioned earlier, better sharpening methods could increase the effectiveness of food processing and medical tools. During this research, efforts can be made to ensure that these improved methods are accessible across the globe.

Economic:

While the goal of this project was to investigate slicing mechanics related to skiing, a better understanding of how sharpening method affects slicing can benefit a wide range of industries. This includes food processing, where a better understanding of sharpening techniques could result in more efficient processing tools and lower production costs. In such a case, certain foods may become more affordable. This would increase the variety of foods people have access to. Additionally, surgical tools can be improved with a better understanding of how sharpening affects the mechanics of slicing. As mentioned under social impact, improved sharpening methods could also increase the effectiveness of surgical tools. This could include longer lasting reusable medical tools. Overall, this could lower the cost of medical procedures, making them more accessible.

References

Atkins, A. G., Xu, X., & Jeronimidis, G. (2004). "Cutting, by pressing and slicing, of thin floppy slices of materials illustrated by experiments on cheddar cheese and salami". Journal of Materials Science, 39(8), 2761–2766. Scopus. https://doi.org/10.1023/B:JMSC.0000021451.17182.86

Brown, C. A., Hansen, H. N., Jiang, X. J., Blateyron, F., Berglund, J., Senin, N., Bartkowiak, T., Dixon, B., Le Goïc, G., Quinsat, Y., Stemp, W. J., Thompson, M. K., Ungar, P. S., & Zahouani, E. H. (2018). Multiscale analyses and characterizations of surface topographies. CIRP Annals, s67(2), 839–862. https://doi.org/10.1016/j.cirp.2018.06.001

Brown C. A. 2023, Personal Communication, *Worcester Polytechnic Institute: Mechanical and Materials Engineering*.

Deibel, Karl-Robert, Christian Raemy, and Konrad Wegener. "Modeling Slice-Push Cutting Forces of a Sheet Stack Based on Fracture Mechanics." Engineering Fracture Mechanics 124–125 (July 2014): 234–47. https://doi.org/10.1016/j.engfracmech.2014.04.029.

Denkena, B., and D. Biermann. "Cutting Edge Geometries." CIRP Annals 63, no. 2 (2014): 631–53. https://doi.org/10.1016/j.cirp.2014.05.009.

Flegel, Dylan and Kern, Richard. "Correlating Microgeometry to Slicing Mechanics: Design of a Simulated Ski Laceration Machine." Worcester Polytechnic Institute, 2022. https://digital.wpi.edu/concern/student_works/7d278x537

Giovannini, Marco, and Kornel Ehmann. "Vibrational Cutting of Soft Tissue with Micro-Serrated Surgical Scalpels." Procedia CIRP 45 (2016): 199–202. https://doi.org/10.1016/j.procir.2016.02.342.

Holden, William M., Michael S. Barnum, Mitchell C. Tarka, Christoph A. Niederhauser, Ryan P. Jewell, and Nathan K. Endres. "Severe Lacerations in Alpine Ski Racing: A Case Series and Review of the Literature." Sports Health: A Multidisciplinary Approach, March 31, 2022, 194173812210765. https://doi.org/10.1177/19417381221076521.

McCarthy, C.T., A. Ní Annaidh, and M.D. Gilchrist. "On the Sharpness of Straight Edge Blades in Cutting Soft Solids: Part II – Analysis of Blade Geometry." Engineering Fracture Mechanics 77, no. 3 (February 2010): 437–51. https://doi.org/10.1016/j.engfracmech.2009.10.003.

McCarthy, C.T., M. Hussey, and M.D. Gilchrist. "On the Sharpness of Straight Edge Blades in Cutting Soft Solids: Part I – Indentation Experiments." Engineering Fracture Mechanics 74, no. 14 (September 2007): 2205–24.

Moronkeji, K., S. Todd, I. Dawidowska, S.D. Barrett, and R. Akhtar. "The Role of Subcutaneous Tissue Stiffness on Microneedle Performance in a Representative in Vitro Model of Skin." Journal of Controlled Release 265 (November 2017): 102–12. https://doi.org/10.1016/j.jconrel.2016.11.004.

N/A. (n.d.). *Code of ethics*. Code of Ethics | National Society of Professional Engineers. (2019) https://www.nspe.org/resources/ethics/code-ethics?gad=1&gclid=EAIaIQobChMI_-iIpeTJ_gIVuWtvBB2zXQ4fEAAYASAAEgL8rvD_BwE

Newman, R. K., & Mahdy, H. (2022, October 8). "Laceration." National Center for Biotechnology Information. Retrieved December 12, 2022, from https://www.ncbi.nlm.nih.gov/books

Soares, Sérgio, Timo Schmid, Lucien Delsa, Nicolas Gallusser, and Beat K. Moor. "Skiing and Snowboarding Related Deep Laceration Injuries. A Five-Season Cross-Sectional Analysis from a Level-1 Trauma Centre in the Swiss Alps." Orthopaedics & Traumatology: Surgery & Research 108, no. 7 (November 2022): 103370. https://doi.org/10.1016/j.otsr.2022.103370.

Stemp J, Macdonald D, Gleason M. "Testing imaging confocal microscopy, laser scanning confocal microscopy, and focus variation microscopy for microscale measurement of edge cross-sections and calculation of edge curvature on stone tools: Preliminary results" Journal of Archaeological Science: Report. (February 2019) https://doi.org/10.1016/j.jasrep.2019.02.010

Tevis D B Jacobs, Till Junge, and Lars Pastewka. “Quantitative characterization of surface topography using spectral analysis” *Surf. Topogr.: Metrol. Prop.* (January 2017) **5** 013001 https://iopscience-iop-org.ezpv7-web-p-u01.wpi.edu/article/10.1088/2051-672X/aa51f8

Appendix A: Slicing Apparatus Code

```
#define dirPin 2
#define stepPin 3
#define numberOfSteps 225
#define stepDuration 2500

void setup() {
  // Declare pins as output:
  pinMode(stepPin, OUTPUT);
  pinMode(dirPin, OUTPUT);
}

void loop() {
  // Set the spinning direction clockwise:
  digitalWrite(dirPin, LOW);

  for (int i = 0; i < numberOfSteps; i++) {
            // These four lines result in 1 step:
            digitalWrite(stepPin, HIGH);
            delayMicroseconds(stepDuration);
            digitalWrite(stepPin, LOW);
            delayMicroseconds(stepDuration);
  }

delay(1000);

  digitalWrite(dirPin, HIGH);
  for (int i = 0; i < numberOfSteps; i++) {
            // These four lines result in 1 step:
            digitalWrite(stepPin, HIGH);
            delayMicroseconds(stepDuration);
            digitalWrite(stepPin, LOW);
            delayMicroseconds(stepDuration);
  }
  while(true){
            digitalWrite(stepPin, LOW);
            digitalWrite(dirPin, LOW);
            }
}
```

Appendix B: Code to Determine Edge Profile in Matlab

```
FileName = input('input file name: '); %input the file name of the measurement
Surface = readmatrix(FileName);
[m,n] = size(Surface);
sampleratey = 2.823480e+03 - 2.820720e+03;
sampleratex = 1224;
MaxRows = round(max(Surface(:,2))/sampleratey);
MaxY = max(Surface(:,2));
dataX = zeros(MaxRows-1,4);
count = 1;
start = 1;
while count ~= MaxRows
   xrange = (count*sampleratex);
   [Z,index] = max(Surface(start:xrange,3));
   dataX(count,1)= index; %x value of highest point in cross section
   dataX(count,2)= Surface(index); %x value of highest point in cross section (um)
   dataX(count,3)= MaxY-(count*sampleratey); %y value of cross section being analyzed
   dataX(count,4)= Z;%corresponding z value of highest point (um)
   count = count+1;
   start = (count-1)*sampleratex;
end
coefficientsX = polyfit(dataX(:,3), dataX(:,2), 1);
yFit = linspace(min(dataX(:,3)), max(dataX(:,3)), max(dataX(:,2)));
xFit = polyval(coefficientsX , yFit);

rotation = round(atand(coefficientsX(1)),4);
if rotation < 0
   CWorCCW = 'clockwise ';
elseif rotation > 0
   CWorCCW = 'counter-clockwise ';
else
   CWorCCW = 'no rotation at ';
end

figure
scatter(dataX(:,2),dataX(:,3),'bo')
hold on
axis([0 3378.24 0 MaxY])
plot(xFit, yFit, 'r-', 'LineWidth', 2);
grid on
legend('Highest Point of Cross-Section','Edge');

values =['Top = ',num2str((xFit(end)/1000)),' mm  Bottom = ', num2str(xFit(1)/1000),' mm'];
disp(' ');
disp('Positions where the edge intercepts the top and bottom of the measurement:');
disp(values);%%To generate a MountainsMap profile, display the location where edge intercepts the top and bottom of the
measurement

disp(' ');
rotdirection = ['Edge should be rotated ',CWorCCW,':'];
disp(rotdirection);
fprintf('%g\n',(abs(rotation)))%%To take perpendicular measurements to the edge, display how the measurement should be rotated
to be a vertical line
disp('degrees');
```

Appendix C: Power Spectral Density (PSD) Measurements

Edge A (EVO sharpened)

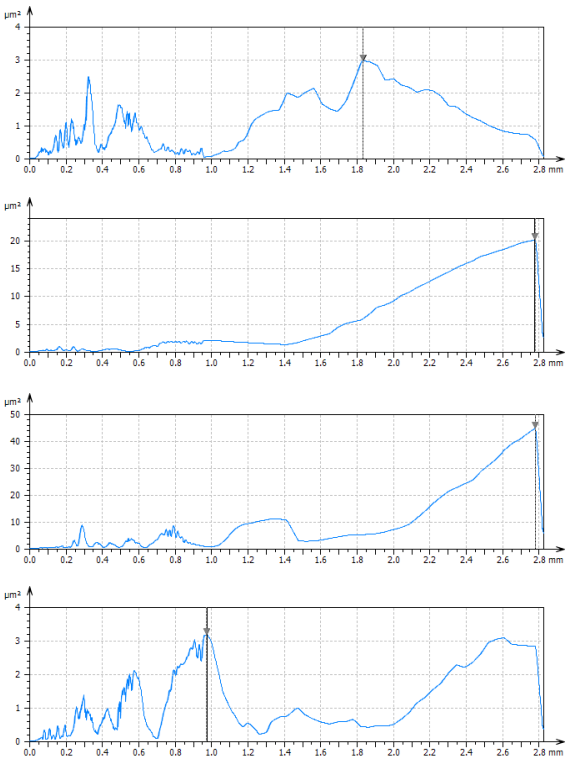
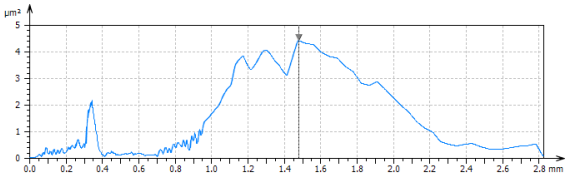

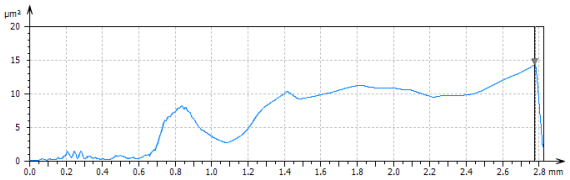

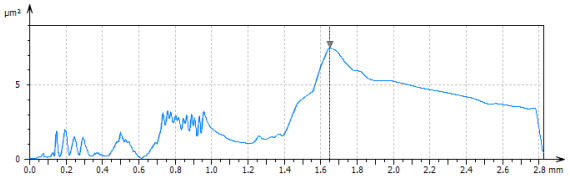

Edge B (EVO sharpened)

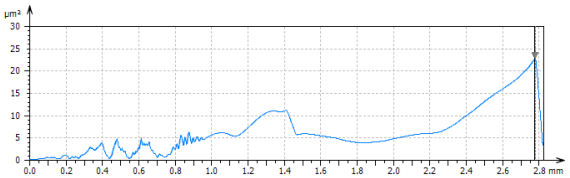
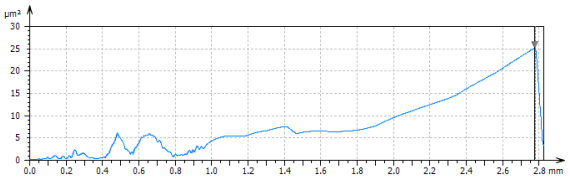
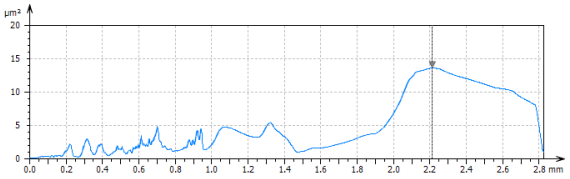
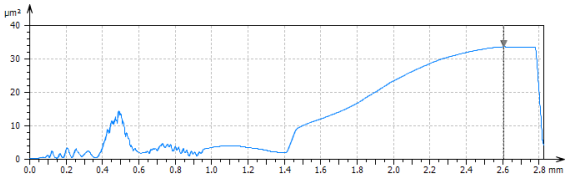
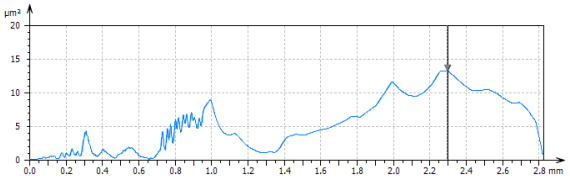
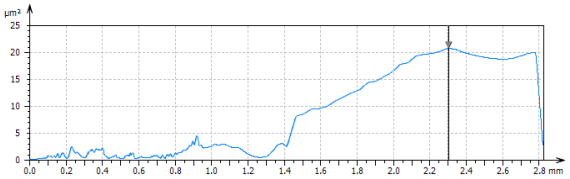
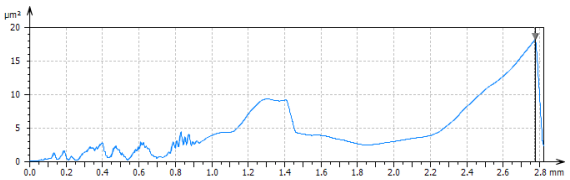

Edge C (EVO sharpened)

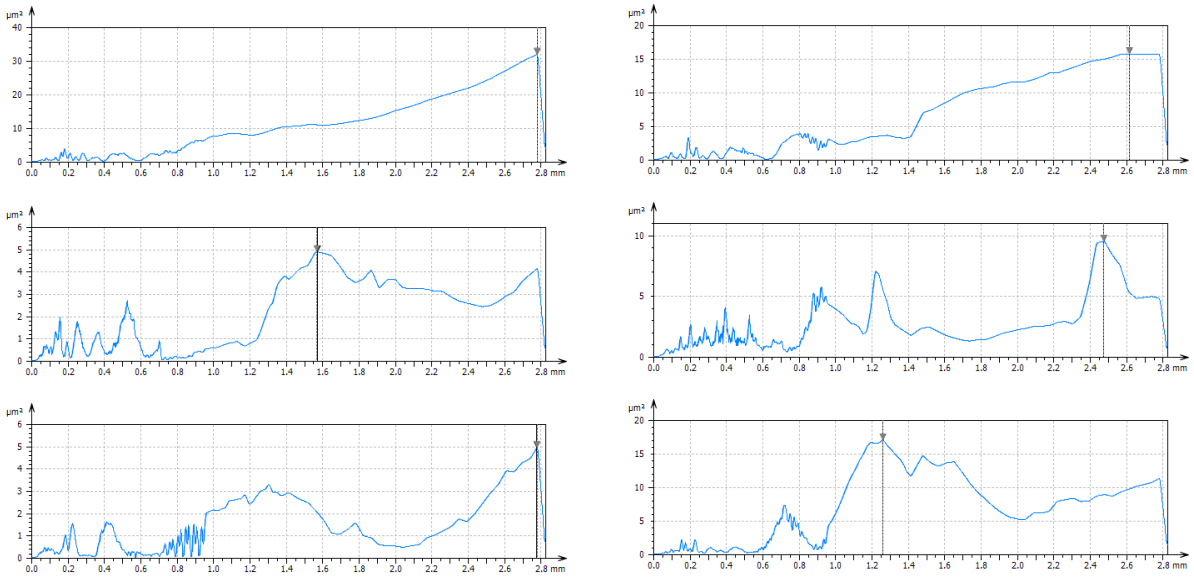

Edge G (EVO sharpened)

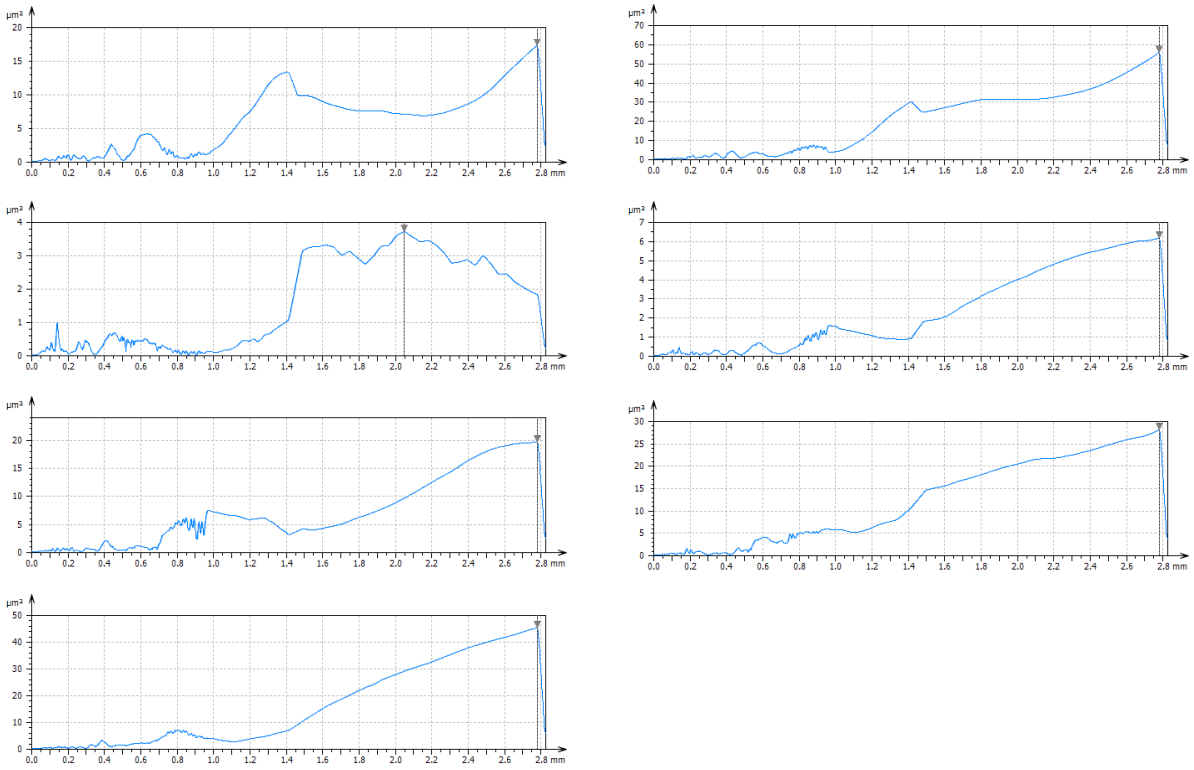

Edge D (Hand sharpened)

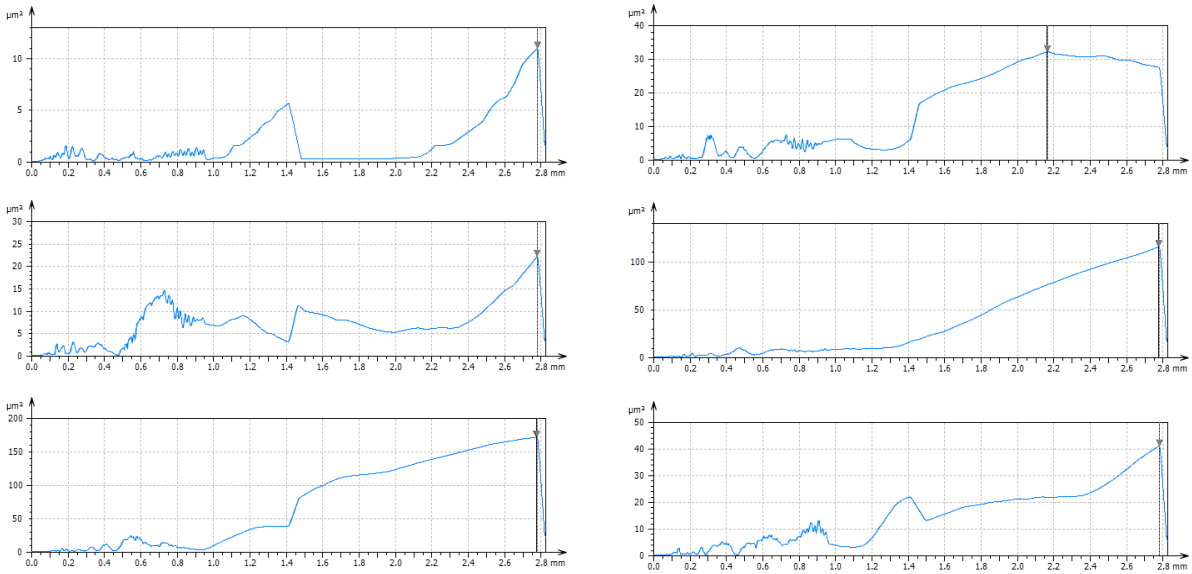

Edge E (Hand sharpened)

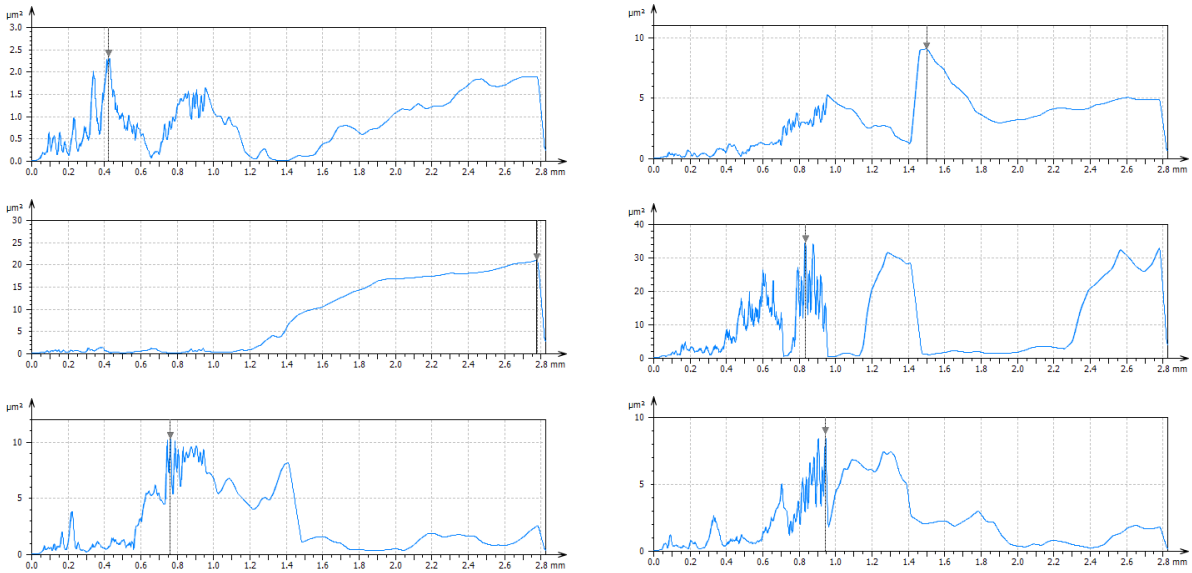

Edge F (Hand sharpened)